

Article

Geochemical Characteristics of Dolomitic Phosphorite Containing Rare Earth Elements and Its Weathered Ore

Shuai Li ¹ , Jie Zhang ², Huaifa Wang ^{1,*} and Caili Wang ¹¹ College of Mining Engineering, Taiyuan University of Technology, Taiyuan 030024, China² Mining College, Guizhou University, Guiyang 550025, China

* Correspondence: wanghuaifa@tyut.edu.cn

Received: 12 April 2019; Accepted: 4 July 2019; Published: 8 July 2019



Abstract: In order to provide a good theoretical guidance for the development and utilization of weathered phosphorite resources, we investigated the geochemical and mineralogical characteristics of primary and weathered phosphorites. The analysis of trace elements showed that the primary ore has hydrothermal sedimentation effect in the later stage, the weathered ore has obvious residual enrichment and the phosphate ore belongs to clastic lithologic phosphate rock. In addition, through leaching test method, it was shown that rare earth elements are present in fluorapatite in the form of isomorphic substitution, and the proportion of rare earth elements adsorbed on clay and other minerals was likely to be between 2% and 3%. The light rare earth elements are relatively enriched in both primary and weathered phosphorite, and Ce and Eu have obvious negative anomalies. The primary phosphorite is a dolomitic phosphorite containing rare earth elements, which are naturally enriched by weathering, and its weathered ore has obvious residual enrichment, while the deposit was characterized by normal marine sedimentation and hydrothermal action.

Keywords: phosphorite; weathered ore; geochemical characteristic; rare earth elements; technological mineralogy

1. Introduction

Phosphorite is a non-renewable resource without substitute and a significant raw material for phosphatic fertilizers and phosphorus-based chemicals [1–3]. There are abundant sedimentary phosphorite deposits in China, most of which were formed in the Neoproterozoic Late Sinian and in the Paleozoic early Cambrian [4,5]. Supergene weathering of these phosphorites produced weathered phosphorite, a potential industrial type of phosphorite, which is a high-quality ore [6]. The formation of weathered phosphorite is restricted and controlled by the geochemical characteristics of primary ore and the external conditions of ore bodies or rock masses presence [7]. Weathering changed the characteristics of phosphorite, and there is a significant difference between weathered ore and primary ore, regardless of their characteristics or grade [8]. Relative to fresh phosphorite, weathered phosphorite is generally enriched in alkali metals, alkaline earth elements, halogen and radioactive elements, and depleted in mantle elements [7,9]. Weathered phosphorites are also characterized by generally enrichment in light rare earth elements (LREE), depletion in HREE, and Eu negative anomaly [10,11].

Different rocks and ores have different resistance to weathering. Carbonate is easier to be weathered and denuded than phosphate, and the weathering products, calcium, and magnesium are easily leached away, residually enriching apatite [12–14]. The phosphorites of Gezhongwu Formation in Zhijin County mainly are bioclast dolomitic and siliceous. The bioclastic components of the phosphorites consist of pelecypods, gastropods, algae, etc [15]. Wang et al. (2004) studied the genesis of the Xinhua phosphorite deposit in Guizhou China and analyzed the REE composition of the ore using ICP-MS [16]. They concluded that phosphorite was formed exclusively by marine sediments

deposited in ancient pericontinental seas. They also suggested that the phosphorite deposit was subjected to strong weathering after deep buried diagenetic processes, which did not change its REE composition remarkably. A systematic study of leaching of rare earths from a phosphorite ore using four leaching modes [17]: sulfuric acid leaching, phosphoric acid leaching, mixed acid leaching, and two-step leaching of phosphoric acid and sulfuric acid was carried out by Jin et al.(2017). Wang (2011) found that the Sr/Ba ratio of weathered phosphorite ores is generally less than 1 due to dissolution of dolomite [7], and the U/Th ratio is generally significantly lower than that of primary phosphorite ores.

Although some geological work has been done on the phosphorite deposits in southern China, the weathered phosphorite has not been fully recognized and studied. In this study, we investigated the mineralogical and geochemical composition of the primary and weathered phosphorites to optimize the use of weathered phosphorite and their rare earth elements in industry.

2. Materials and Methods

2.1. Materials

Six phosphorite samples from different locations in the Zhijin mining district in the Guizhou Province, China, were analyzed for their major oxides and trace elements composition, using the lithium borate/lithium metaborate and X spectrofluorimetry methods [18,19]. The assay results are summarized in Table 1. The samples 1 and 2 are form primary phosphorites and samples 3 to 6 are form weathered phosphorites according to the weathered phosphorite criteria proposed by Zhang et al. [6,20].

Table 1. Major oxides (%) and trace elements(ppm) of the studied phosphorite samples.

Oxides	Phosphorite					
	Primary			Weathered		
	Sample No.					
	1	2	3	4	5	6
P ₂ O ₅	19.36	9.42	30.12	29.21	31.01	35.18
SiO ₂	13.61	24.95	17.59	18.29	17.69	10.15
Al ₂ O ₃	1.57	1.71	4.25	4.75	2.91	2.23
Fe ₂ O ₃	0.99	0.95	3.28	3.49	2.74	1.98
CaO	35.75	26.98	38.73	37.59	39.51	44.72
MgO	7.79	10.36	0.55	0.61	0.54	0.27
Na ₂ O	0.06	0.07	0.08	0.08	0.06	0.09
K ₂ O	0.42	0.53	1.13	1.27	0.90	0.57
TiO ₂	0.08	0.05	0.12	0.13	0.12	0.11
L.O.I	18.50	23.70	3.90	4.06	3.33	2.78
Total	98.13	98.72	99.75	99.48	98.81	98.08
Trace Elements (ppm)						
Ba	183	3200	433	479	732	455
Ce	142	78	247	232	210	272
Cr	20	20	40	40	50	40
Cs	1	1	2	2	2	1
Dy	27	14	46	44	42	53
Er	15	8	26	25	24	29
Eu	6	4	10	10	13	14
Ga	4	3	9	10	7	6
Gd	34	18	58	55	53	69
Hf	1	1	2	2	1	2
Ho	6	3	10	9	9	11
La	207	103	370	353	288	406
Lu	1	1	2	2	2	2
Nb	2	2	4	4	2	2
Nd	150	81	258	241	227	307
Pr	35	19	62	58	52	72

Table 1. Cont.

Trace Elements (ppm)						
Rb	9	8	27	28	19	14
Sm	27	14	45	42	41	54
Sn	1	1	1	1	1	1
Sr	679	335	677	722	698	1305
Tb	5	2	8	7	7	9
Th	7	5	9	9	5	9
Tm	2	1	3	3	3	3
U	5	3	10	9	18	11
V	19	8	33	32	72	24
W	2	2	2	2	1	3
Y	317	166	566	538	518	602
Yb	8	5	14	14	13	16
Zr	49	37	74	66	44	54
U/Th	0.64	0.57	1.03	1.01	3.55	1.11
Sr/Ba	3.72	0.10	1.56	1.51	0.95	2.87
Rb/Cs	14.92	10.25	15.46	14.71	10.32	16.63
Zr/Hf	37.69	37.00	35.24	31.43	33.85	31.76

2.2. Methods

2.2.1. X-ray Diffraction (XRD) Analysis

In order to identify the mineral composition of phosphorite samples, an X-ray powder diffractometer (Rigaku D/MAX 2500, Tokyo, Japan) was applied by using Cu K α radiation (40 kV, 100 mA). The samples were scanned at the speed of 6°/min over a 2 θ range of 2.6–45°. Furthermore, SIROQUANT software (V3, Sietronics) was carried out to quantify the mineralogical composition. The software used the full-profile Rietveld method to refine the shape of calculated XRD pattern against the profile of a measured pattern [21].

2.2.2. Optical Microscopy

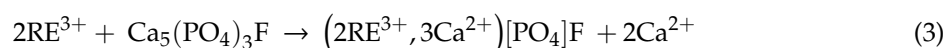
Thin section of phosphorite samples were prepared and investigated by optical microscopy [22,23]. An Olympus CX21 polarizing microscope was used to investigate the mineral characteristics and textural relationships of phosphorite.

2.2.3. SEM-EDX

The morphology, composition, and orientation of phosphorites were studied using a Hitachi 3400 N scanning electron microscope (SEM) in Guizhou University Physical and Chemical Testing Center lab. The morphology was studied using back scattered electrons (BSE) and the composition of the various phases using EDX [24–26].

2.3. Leaching Test

In order to determine the presence of REE, phosphorite samples were leached with different acids and inorganic salts [17]. A 10 g composite sample was leached with acid (HCl or HNO₃) and whereas a 5 g composite samples was leached with inorganic salt. The experiments were carried out at room temperature for 2 h in 100 mL leaching agent with acids concentrations of 1%, 3%, 5%, 7%, 9%, and 11% and inorganic salts concentrations of 5%, 10%, 15%, 20%, and 25%. The main reactions can be summarized as follows [27]:



The four leaching agents were hydrochloric acid (HCl), nitric acid (HNO₃), ammonium chloride (NH₄Cl) and sodium chloride (NaCl). HCl and HNO₃, both with an analytical purity, were purchased from Chongqing Chuandong Chemical (Group) Co., Ltd. (Chongqing, China); while the other reagents were obtained from Tianjin Kemiou Chemical Reagent Co., Ltd. (Tianjin, China).

2.4. Mathematical Method for Judging Independent Minerals

Independent minerals, concentrated state of elements, are particles larger than 0.001 mm in diameter and can be studied with naked eyes or under the microscope. There are two basic conditions for the formation of independent minerals [17]: one is relative stability under certain physical and chemical conditions; the other is certain element content. It is necessary to carry out mathematical analysis on the content of phosphorus and rare earth elements in the phosphate rock and calculate their mean value and mean variance. If the ratio of the mean value and mean variance of the two are significantly different (generally considered to be 20%), rare earth will exist in the form of independent mineral; otherwise, it will exist in a dispersed form such as homogeneity, adsorption, etc.

When a dependent variable, y , varies to some extent with an independent variable, x , it can be assumed that they have the following relationship: $y = a + bx$. According to the analysis in Table 1, we let y be the content of rare earth elements and x be the content of phosphorus pentoxide. The regression equation was established, and the coefficients a and b were obtained using Equations (4–8).

$$b = \frac{\sum (x_i - \bar{x})(y_i - \bar{y})}{\sum (x_i - \bar{x})^2} \quad (4)$$

$$a = \bar{y} - b\bar{x} \quad (5)$$

$$\bar{x} = \frac{1}{N_{sa}} \sum x_i \quad (6)$$

$$s_x = \sqrt{\frac{\sum (x_i - \bar{x})^2}{N_{sa} - 1}} \quad (7)$$

$$s_y = \sqrt{\frac{\sum (y_i - \bar{y})^2}{N_{sa} - 1}} \quad (8)$$

where \bar{y} and \bar{x} are the mean values of dependent variable y and independent variable x , respectively; s_x and s_y are the mean square deviation of x and y , respectively; N_{sa} is total number of samples.

3. Results and Discussion

3.1. Comparison of Mineral Composition between Primary Weathered Phosphorites

All the samples are rich in CaO, P₂O₅ and SiO₂ (Table 1). The L.O.I in primary phosphorite is higher than in weathered ore. Fluorapatite is present in both primary and weathered ores, with respective averages of 31.7% and 79.3% (Figure 1). Dolomite was detected only in primary ore with an average content of 48.75% (Figure 1 no. 1 and 2).

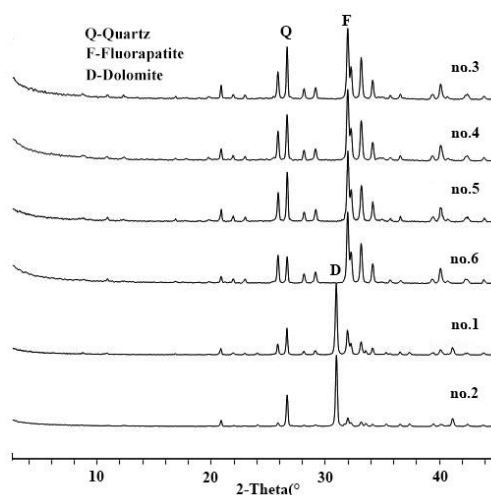


Figure 1. X-ray diffraction (XRD) patterns of studied phosphorite samples.

3.2. Ore Texture Differences

Figure 2 shows the distribution and textural characteristics of various minerals present in the ore. The composition of the various minerals was studied with a SEM equipped with an EDX detector (Figure 3) [28,29]. The results showed that fluorapatite, embedded in dolomitic matrix, is the main phosphorus-bearing mineral. Fluorapatite occurs in spherical, oolitic, and clastic forms, in mainly grey-yellow and grey-brown colors under transmitted light. Dolomite is the main cement in the rock and is colorless or white under plane parallel light. Dolomite also appears in the matrix of phosphorite as euhedral and subhedral isolated crystals and aggregate. Quartz was randomly distributed in the dolomite matrix, with a few crystals disseminated in phosphorite. It occurs as granular and hypidiomorphic grains with clean surfaces.

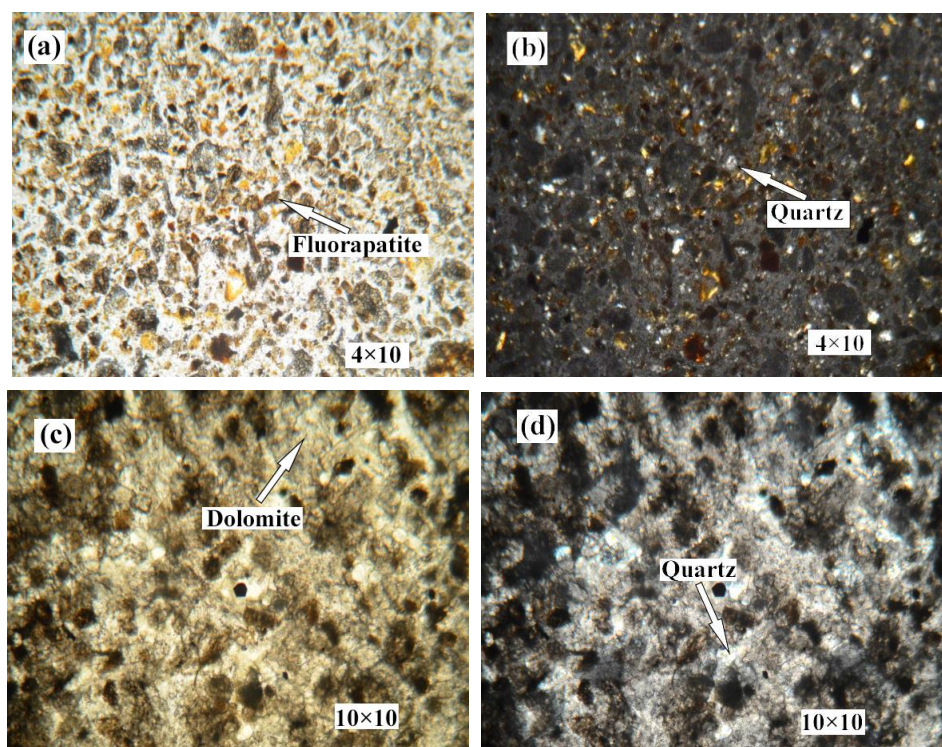


Figure 2. Cont.

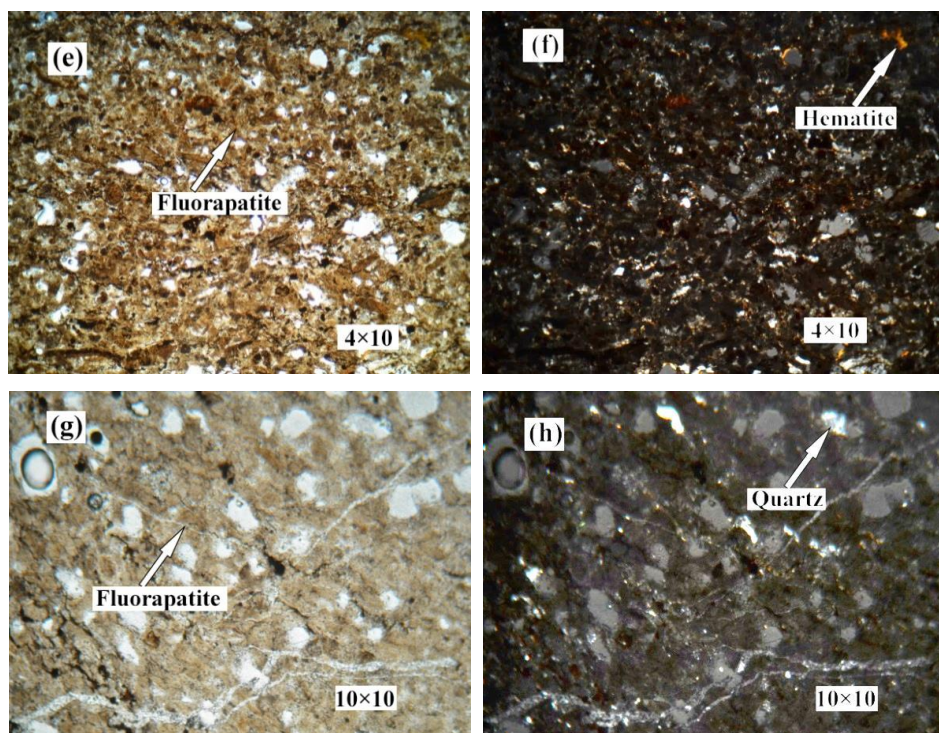


Figure 2. Photomicrographs of phosphorite. (a) no.1 crossed nicols. (b) no.1 perpendicular polarized light. (c) no.2 plane polarized light. (d) no.2 crossed nicols. (e) no.4 plane polarized light. (f) no.4 crossed nicols. (g) no.5 plane polarized light. (h) no.5 crossed nicols.

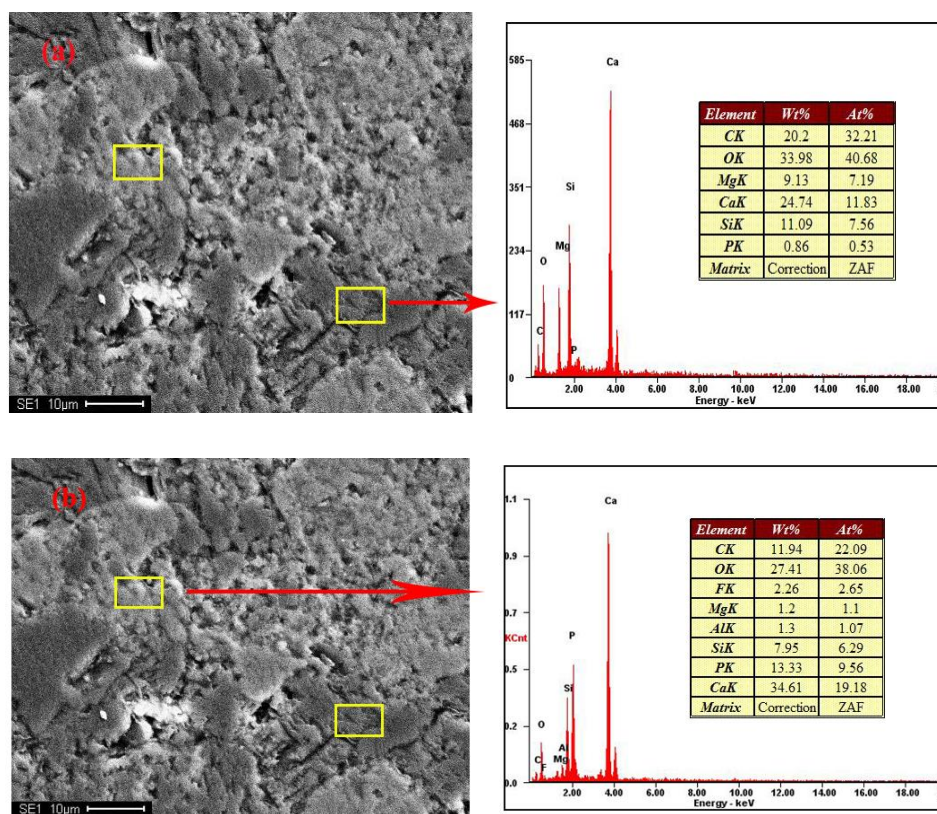


Figure 3. Cont.

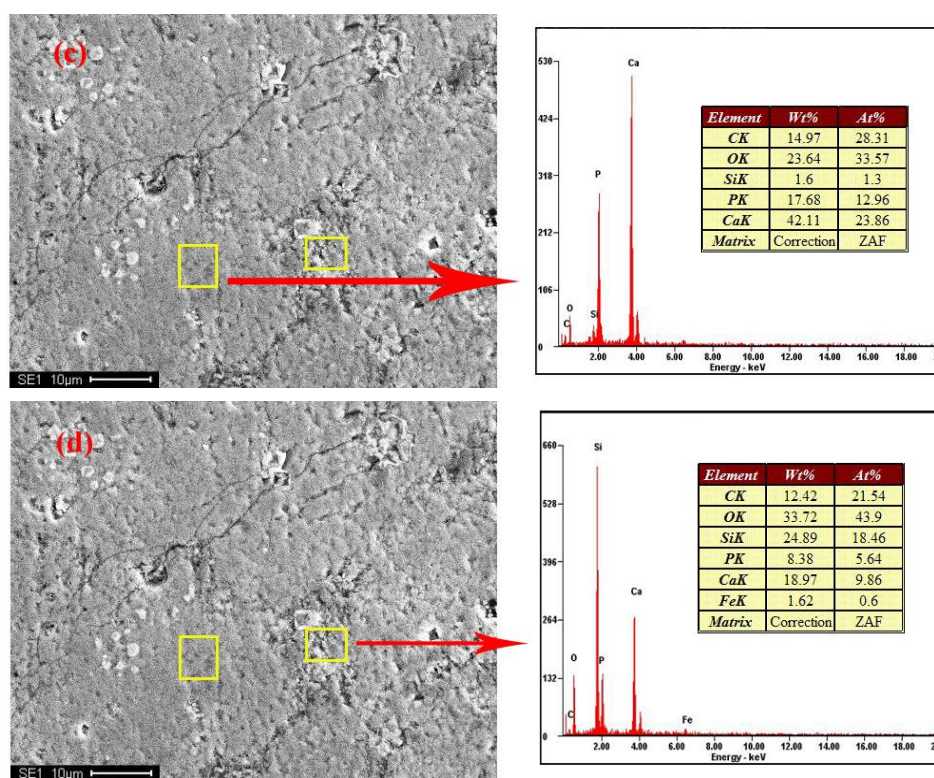


Figure 3. SEM-EDX results of samples. (a,b) no.1; (c,d) no.4.

3.3. Comparison of Trace Elements

As shown in Table 1, the primary and weathered ores are enriched in Ba, Ce, La, Nd, Sr, and Y, and depleted in Co and Ni. Gallium, a chalcophile element related to hydrothermal activity [22], was enriched in the weathered ore and gradually depleted with the increase in temperature. Chromium, a siderophile element mainly found in ultrabasic and basic rocks, was also enriched in the weathered ore and mainly found in basic rocks and ultrabasic rocks.

U and Th are lithophile elements with similar geochemical properties, and they usually occur in oxides or oxygen-bearing salts [19]. U/Th values (see Table 1) of primary ore are lower than 1, while those of weathered ore are higher than 1, which indicates that hydrothermal precipitation has an effect on the later stage of primary ore, and weathered ore has obvious residual enrichment properties. The average Sr/Ba values (Table 1) of primary and weathered ores are all greater than 1 except for sample No.6, indicating that the phosphate rock is clastic in origin. The mean Rb/Cs values of primary ore and weathered ore were almost the same, indicating that these active lithophile elements were adsorbed or bound evenly in the minerals of the original rock. Both Zr and Hf are high field strength elements and indicate differences in hydrothermal action, the former was enriched at an early stage while the latter at a later stage. The Zr/Hf value of weathered ore was significantly smaller than that of primary ore, indicating that primary ore was related to the early hydrothermal activity while weathered ore was relevant to the later stage.

3.4. Comparison of Rare Earth Elements

As shown in Table 2, the content of total rare earth elements in weathered phosphate rock was higher than that in primary ore. Concentration of LREE is higher than that of HREE in both types of ore (average LREE/HREE ratio = 1.35, average (La/Yb)_N ratio = 16.11), and δCe and δEu are obtained using Equations (9) and (10). Figure 4 shows negative Ce and Eu anomalies in primary and weathered ores, while La, Nd and Y are relatively enriched. The negative Ce anomaly indicates that there may be two situations: one is that the ore-forming environment of phosphate rock was oxidizing and Ce^{4+} with

small ion radius was difficult to enter apatite lattice to form a loss; the other is that Ce^{4+} can easily form CeO_2 which lead to loss during the reworking of phosphate rock in marine environment. The negative Eu anomalies indicate that magma was differentiated by a certain intensity of crystallization [14–17]. In summary, the characteristics of REE indicated that the phosphorite belongs to the normal marine sedimentary rock.

$$\delta Ce = Ce_N / (La_N \times Pr_N)^{0.5} \tag{9}$$

$$\delta Eu = Eu_N / (Sm_N \times Gd_N)^{0.5} \tag{10}$$

Table 2. Rare earth elements(ppm) of phosphorite.

REE	Primary Phosphorite			Weathered Phosphorite		
	Sample No.					
	1	2	3	4	5	6
La	207	102.5	370	353	288	406
Ce	142	78.3	247	232	210	272
Pr	35.4	19.1	61.6	58.1	52	72.1
Nd	149.5	80.6	258	241	227	307
Sm	26.6	14.5	45.4	42.2	41.1	54.3
Eu	6.34	3.65	10.45	9.89	12.6	14
Gd	33.8	18.45	57.6	54.8	52.8	69.1
Tb	4.55	2.48	7.78	7.35	7.02	9.05
Dy	27	14.3	46.2	43.7	41.7	53
Ho	5.63	3.04	9.86	9.33	9	11.25
Er	14.65	8.05	26	24.7	23.7	29.1
Tm	1.71	0.97	2.98	2.85	2.69	3.28
Yb	8.43	4.76	14.35	13.75	12.8	16.25
Lu	1.13	0.67	1.87	1.81	1.65	2.08
Y	317	165.5	566	538	518	602
ΣREE	980.74	516.82	1725.09	1632.48	1500.06	1920.51
LREE	566.84	298.6	992.45	936.19	830.7	1125.4
HREE	413.9	218.22	732.64	696.29	669.36	795.11
LREE/HREE	1.37	1.37	1.35	1.34	1.24	1.42
(La/Yb) _N	16.37	14.36	17.19	17.12	15	16.66
δEu	0.64	0.68	0.62	0.63	0.82	0.70
δCe	0.36	0.39	0.35	0.35	0.38	0.35

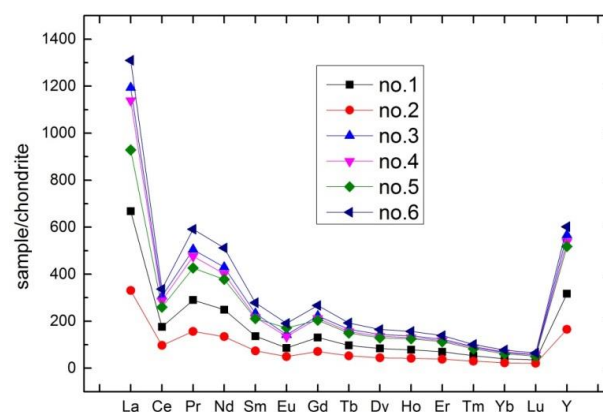


Figure 4. Normalized rare earth elements (REE) patterns of phosphorite samples (after Boynton, 1984 [30]).

3.5. Analysis of Rare Earth Elements (REE) Occurrence State

3.5.1. Analysis of Independent Form

After calculation, the average values $\bar{x} = 25.7170$ and $\bar{y} = 0.1379$, the mean square errors $s_x = 9.5433$ and $s_y = 0.0528$, and the regression equation $y = 0.0054x - 0.0019$ were obtained. As a

consequence, the values $\left(\frac{\bar{x}}{y}\right) = 186.451$ and $\left(\frac{s_x}{s_y}\right) = 180.747$ were also acquired, and they differ by 3.06%, which is much less than 20%. Therefore, it is considered that the rare earth elements are unlikely to exist as an independent mineral [15,31,32].

3.5.2. Analysis of Isomorphous Form

Rare earth elements can either exist in the form of independent minerals or isomorphous substitution in the minerals' lattices. If the REE exists in the form of a separate mineral such as monazite and xenotime, it is difficult to dissolve in the dilute acid, even in small amounts. If the rare earth elements exist in the crystal lattice of colloidal phosphate ore, their physicochemical properties should be similar, the rare earth elements can be completely dissolved in dilute acid together with the colloidal phosphate [31]. Therefore, under certain conditions, the fluorapatite in phosphorite can be dissolved by dilute acid, and the leaching rate of phosphorus and rare earth elements can be analyzed to study the department of rare earth elements [31].

The leaching process (see Equations (1)–(3)) was carried out using a magnetic stirrer at room temperature. It can be seen from Figure 5 that the leaching rates of phosphorus and rare earth are approximately the same. When the leaching rate reaches 99.98%, it no longer increases with increase of acid concentration, meaning they exist in the form of isomorphism. With the dissolution and lattice destruction of apatite, phosphorus and rare earth elements were transferred into the solution at the same time. The isomorphous substitution involves the replacement of Ca^{2+} in apatite by REE [31].

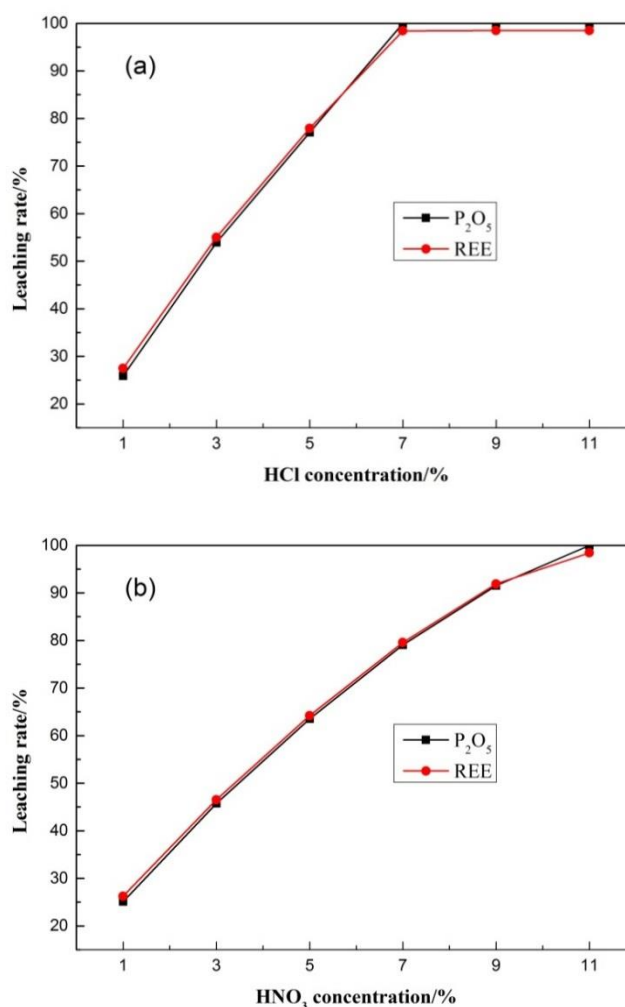


Figure 5. Results of acid leaching test. (a) HCl leaching test; (b) HNO₃ leaching test.

3.5.3. Analysis of Ion Adsorption Form

If rare earth elements are adsorbed on clays or other minerals, they (REE) can generally be leached out by inorganic salts [33–35]. In this experiment, a 5 g composite sample was leached with NH_4Cl and NaCl for 2 h in 100 mL inorganic salts with different concentrations and the results are shown in Figure 6. The leaching rate of rare earth increases slowly with increasing concentration of inorganic salts until at 2.6%, which indicates a low amount of adsorbed REE. Taking into account experimental errors, its content is likely to be between 2% and 3% [33–36].

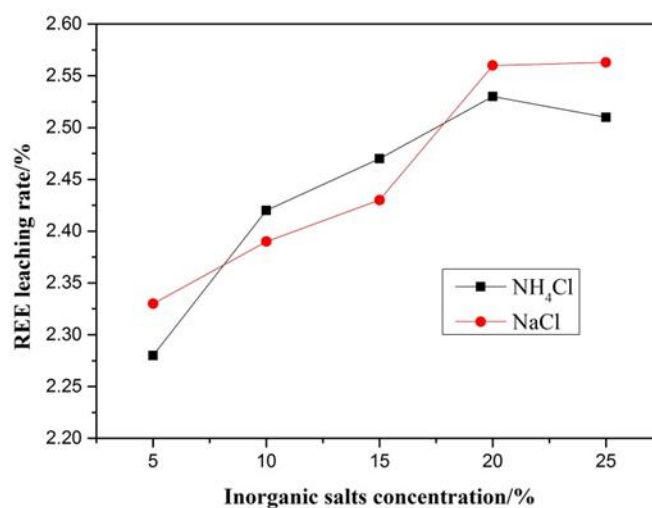


Figure 6. Results of inorganic salts leaching test.

4. Conclusions

The weathering of primary phosphorite in southern China increases the concentration of P_2O_5 , Fe_2O_3 , and Al_2O_3 , and decreases the MgO , CaO , and CO_2 content. The concentration of trace elements including Ba, Ce, La, Nd, Sr, and Y was also increased, while the Co and Ni content was strongly depleted, indicating the inheritance from the original rocks. The U/Th ratios indicate that the primary ore was affected by hydrothermal imprint in the later stage of sedimentation, and the weathered ore was residually enriched in REE. Light rare earth elements are enriched relative to HREE in both primary and weathered ores, and Ce and Eu both have negative anomalies. The REE occurs mainly in fluorapatite crystal lattice and in isomorphic substitution with Ca, with only a small proportion (2–3%) adsorbed onto the mineral surface. Their ability to form separate minerals is low. The characteristics of rare earth elements indicated that the phosphorite deposits are normal marine sedimentary rocks.

Author Contributions: The contributions of the authors were as follows: conceptualization, J.Z. and S.L.; methodology, J.Z. and S.L.; validation, S.L., J.Z., H.W. and C.W.; investigation, J.Z. and S.L.; resources, J.Z. and S.L.; data curation, S.L.; writing—original draft preparation, S.L.; writing—review and editing, S.L.; visualization, S.L.; supervision, C.W.; project administration, J.Z.; funding acquisition, H.W.

Funding: This research was funded by the National Natural Science Foundation of China, grant number 51164004, and the APC was funded by Huaifa Wang.

Acknowledgments: Thanks for the software and formal analysis provided by Aoshi Analytical Testing (Guangzhou, China) Co., Ltd.

Conflicts of Interest: The authors declare no conflict of interest.

References

1. Abouzeid, A.Z.A. Physical and thermal treatment of phosphate ores—An overview. *Int. J. Miner. Process.* **2008**, *85*, 59–84. [[CrossRef](#)]
2. dos Santos, M.A.; Santana, R.C.; Capponi, F.; Ataide, C.H.; Barrozo, M.A.S. Effect of ionic species on the performance of apatite flotation. *Sep. Purif. Technol.* **2010**, *76*, 15–20. [[CrossRef](#)]

3. Gharabaghi, M.; Irannajad, M.; Noaparast, M. A review of the beneficiation of calcareous phosphate ores using organic acid leaching. *Hydrometallurgy* **2010**, *103*, 96–107. [[CrossRef](#)]
4. Lin, Y. *The Construction and Application of Phosphorus Resource Development and Utilization Model in China*; Hefei University of Technology: Hefei, China, 2010.
5. Zhang, W.; Ma, W.; Zhang, F.; Ma, J. Comparative analysis of the superiority of China's phosphate rock and development strategies with that of the United States and Morocco. *J. Nat. Resour.* **2005**, *20*, 378–386.
6. Li, T.; Wen, S.; Tian, P.; Tang, Z.; Huang, Y. Weathered phosphorites in south China. *Geol. Chem. Miner.* **1996**, *3*, 53–57.
7. Wang, J. *Study on Geology and Geochemistry of Weathered Phosphate Deposits, South China*; China University of Geosciences: Beijing, China, 2011.
8. Chang, S.; Zhu, J.; Liu, Y.; He, J. Study status and trends of weathered phosphate rocks in Yunnan, Guizhou. *Ind. Miner. Process.* **2010**, *39*, 41–44.
9. Tian, S.; Wang, Q.; Zhu, H.; Zhu, Y.; Zhou, J.; Wang, J. Fixed quantity exploration and assessment of weathered phosphoric ore in southwest of China. *Geol. Chem. Miner.* **2004**, *4*, 205–209.
10. Wei, D.; Cui, X. Study on process characteristic of heavy rare earths in phosphorite in Guizhou province. *Conserv. Util. Miner. Resour.* **2003**, *2*, 38–40.
11. Yang, R.D.; Gao, H.; Wang, Q.; Bao, M. REE enrichment in Early Cambrian Gezhongwu formation phosphorous rock series in Sanjia, Zhijun County, Guizhou Province, China. *J. Rare Earths* **2005**, *23*, 760–767.
12. Ross, J.; Gao, L.; Meouch, O.; Anthony, E.; Sutarwala, D.; Mamo, H. Carbonate Apatite Precipitation from Synthetic Municipal Wastewater. *Minerals* **2017**, *7*, 129. [[CrossRef](#)]
13. Salama, W.; Khirekesh, Z.; Amini, A.; Bafti, B.S. Diagenetic evolution of the upper Devonian phosphorites, Alborz for Mountain Range, northern Iran. *Sediment. Geol.* **2018**, *376*, 90–112. [[CrossRef](#)]
14. Zhang, J.; Shun, C.; Yang, G.; Xie, F. Separation and enrichment of rare earth elements in phosphorite in Xinhua, Zhijin, Guizhou. *J. Rare Earths* **2006**, *24*, 413.
15. Shi, C.; Hu, R.; Wang, G. Study on REE geochemistry of Zhijin phosphorites, Guizhou province. *J. Mineral. Petrol.* **2004**, *24*, 71–75.
16. Wang, M.; Sun, X.; Ma, M. Rare earth elements geochemistry and genesis of Xinhua large-size phosphorite deposit in western Guizhou. *Miner. Depos.* **2004**, *23*, 484–493.
17. Jin, H.-X.; Wu, F.-Z.; Mao, X.-H.; Wang, M.-L.; Xie, H.-Y. Leaching isomorphism rare earths from phosphorite ore by sulfuric acid and phosphoric acid. *Rare Met.* **2017**, *36*, 840–850. [[CrossRef](#)]
18. Lednev, A.V.; Lozhkin, A.V. Remediation of agrosoddy-podzolic soils contaminated with cadmium. *Eurasian Soil Sci.* **2017**, *50*, 620–629. [[CrossRef](#)]
19. Li, J.; Jin, H.; Chen, Y.; Mao, X. Rare earth elements in Zhijin phosphorite and distribution in two-stage flotation process. *J. Rare Earths* **2007**, *25*, 85–90.
20. Zhang, J. The weathered ore criterion of Dianchi phosphorite. *Yunnan Metall.* **1992**, 24–30.
21. Li, X.; Zhang, Q.; Hou, B.; Ye, J.; Mao, S.; Li, X. Flotation separation of quartz from collophane using an amine collector and its adsorption mechanisms. *Powder Technol.* **2017**, *318*, 224–229. [[CrossRef](#)]
22. Gao, P.; He, Z.; Li, S.; Lash, G.G.; Li, B.; Huang, B.; Yan, D. Volcanic and hydrothermal activities recorded in phosphate nodules from the Lower Cambrian Niutitang Formation black shales in South China. *Palaeogeogr. Palaeoclimatol. Palaeoecol.* **2018**, *505*, 381–397. [[CrossRef](#)]
23. Huggett, J.; Hooker, J.N.; Cartwright, J. Very early diagenesis in a calcareous, organic-rich mudrock from Jordan. *Arab. J. Geosci.* **2017**, *10*, 270. [[CrossRef](#)]
24. Breiland, A.A.; Flood, B.E.; Nikrad, J.; Bakarich, J.; Husman, M.; Rhee, T.; Jones, R.S.; Bailey, J.V. Polyphosphate-Accumulating Bacteria: Potential Contributors to Mineral Dissolution in the Oral Cavity. *Appl. Environ. Microbiol.* **2018**, *84*. [[CrossRef](#)] [[PubMed](#)]
25. Chen, J.; Yang, R.; Wei, H.; Gao, J. Rare earth element geochemistry of Cambrian phosphorites from the Yangtze Region. *J. Rare Earths* **2013**, *31*, 101–112. [[CrossRef](#)]
26. Gamez Vintaned, J.A.; Linan, E.; Navarro, D.; Zhuravlev, A.Y. The oldest Cambrian skeletal fossils of Spain (Cadenas Ibericas, Aragon). *Geol. Mag.* **2018**, *155*, 1465–1474. [[CrossRef](#)]
27. Walawalkar, M.; Nichol, C.K.; Azimi, G. Process investigation of the acid leaching of rare earth elements from phosphogypsum using HCl, HNO₃, and H₂SO₄. *Hydrometallurgy* **2016**, *166*, 195–204. [[CrossRef](#)]

28. Linsy, P.; Nath, B.N.; Mascarenhas-Pereira, M.B.L.; Vinitha, P.V.; Ray, D.; Babu, C.P. Benthic cycling of phosphorus in the Eastern Arabian Sea: Evidence of present day phosphogenesis. *Mar. Chem.* **2018**, *199*, 53–66. [[CrossRef](#)]
29. Sinirkaya, M.; Ozer, A.K.; Gulaboglu, M.S. Kinetics of dissolution of Mardin-Mazidagi (Turkey) phosphate ore in dilute phosphoric acid solutions. *Miner. Metall. Process.* **2010**, *27*, 110–115. [[CrossRef](#)]
30. Boynton, W.V. Cosmochemistry of the Rare Earth Elements. In *Rare Earth Element Geochemistry*; Henderson, P., Ed.; Elsevier: Amsterdam, The Netherlands, 1984.
31. Xie, F.; Zhang, T.A.; Dreisinger, D.; Doyle, F. A critical review on solvent extraction of rare earths from aqueous solutions. *Miner. Eng.* **2014**, *56*, 10–28. [[CrossRef](#)]
32. Zhang, J.; Zhang, Q.; Chen, D. REE geochemistry of the ore-bearing REE in Xinhua phosphorite, Zhijin, Guizhou. *J. Mineral. Petrol.* **2003**, *23*, 35–38.
33. Baghdady, A.R.; Howari, F.M.; Al-Wakeel, M.I. On the mineral characteristics and geochemistry of the Florida phosphate of Four Corners and Hardee County mines. *Sediment. Geol.* **2016**, *342*, 1–14. [[CrossRef](#)]
34. Chen, J.; Yang, R.; Zhang, J. Mode of occurrence of rare earth elements in phosphorite in Zhijin county, Guizhou province, China. *Acta Mineral. Sin.* **2010**, *30*, 123–129.
35. Gall, Q.; Davis, W.J.; Lowe, D.G.; Dabros, Q. Diagenetic apatite character and in situ ion microprobe U-Pb age, Keeseville Formation, Potsdam Group, New York State. *Can. J. Earth Sci.* **2017**, *54*, 785–797. [[CrossRef](#)]
36. Huang, X.-W.; Long, Z.-Q.; Wang, L.-S.; Feng, Z.-Y. Technology development for rare earth cleaner hydrometallurgy in China. *Rare Met.* **2015**, *34*, 215–222. [[CrossRef](#)]



© 2019 by the authors. Licensee MDPI, Basel, Switzerland. This article is an open access article distributed under the terms and conditions of the Creative Commons Attribution (CC BY) license (<http://creativecommons.org/licenses/by/4.0/>).